

THE AMERICAN MINERALOGIST

JOURNAL OF THE MINERALOGICAL SOCIETY OF AMERICA

Vol. 36

SEPTEMBER-OCTOBER, 1951

Nos. 9 and 10

THERMAL STUDY OF THE CA-MG-Fe CARBONATE MINERALS*

J. LAURENCE KULP, PURFIELD KENT, AND PAUL F. KERR,
Columbia University, New York, N. Y.

CONTENTS

Abstract

- I. Introduction
- II. Experimental procedure
- III. Effects of particle size and diluent on DTA curves.
- IV. Data of Ca-Mg-Fe carbonate minerals
 - A. Calcite
 - B. Siderite
 - C. Magnesite
 - D. Dolomite-Ankerite
 - E. Natural carbonate aggregates
- V. Discussion
- References

ABSTRACT

Differential thermal analyses have been made of a large number of natural carbonate minerals in the Ca-Fe-Mg composition triangle. The characteristics of the thermal behaviour of these minerals and the related structural changes have been investigated and defined. X-ray diffraction and chemical analysis were used to identify structural phases and substitution phenomena in the group. Substitution in calcite, magnesite, siderite, dolomite, and ankerite is readily detected by thermal studies. It is possible to quantitatively estimate the concentrations of each of these common carbonate minerals in a natural aggregate and to estimate the amount of substitution in each phase. Evidence for complete ionic substitution between the pairs Ca-Mn, and Fe-Mg, now seems clear. Between Ca-Mg and Ca-Fe, however, the amount of substitution in a calcite type lattice is very limited. Complete substitution between Fe and Mn, and between Mg and Mn appears possible but is not completely represented in minerals.

I. INTRODUCTION

The carbonates of calcium, magnesium, and ferrous iron occur under various geologic conditions. While the atomic architecture of the minerals which these cations form has been known for some time (Bragg, 1937), these studies were only concerned with the relatively pure single crystals. The natural occurrence of carbonate aggregates is often highly complex. Differential thermal analysis (DTA) appeared to offer a means of

* Contribution No. 37, Lamont Geological Observatory.

defining the fraction of each mineral lattice present in such mixtures and the concentration of each cation in each lattice. The correlation of the thermal data with the structural pattern should provide a broader understanding of these minerals in their natural occurrence. In addition, these data may contribute to a better understanding of such widely different occurrences as the siderite iron ores, carbonate mineralization associated with hydrothermal deposits and petroliferous sediments.

The focus of this study lies in the ankerite area of the Ca-Fe-Mg composition triangle. In order to adequately interpret the data on ankerite, it was desirable to do some preliminary work on the simple carbonates. Some of these minerals have been described in the DTA literature. Beck (1950), Cuthbert and Rowland (1947), and Kerr and Kulp (1948) have made reconnaissance DTA studies on one or two specimens of various common carbonates. Fredrickson (1948), Rowland and Jonas (1949), and Kerr and Kulp (1947) have published more detailed work on siderite. Faust (1950) has done a careful study of calcite and aragonite and has published some thermal work on dolomite and magnesite (Faust, 1944, 1949). Kulp, Wright, and Holmes (1949) made a thermal study of the closely related rhodochrosite and the substitution phenomena from rhodochrosite to calcite. No extensive DTA work has appeared on ankerite or the synthesis of the thermal relationships in the common carbonates.

The authors wish to acknowledge the assistance of H. Adler, H. Glass, and P. K. Hamilton in the experimental work. They are particularly grateful to Mr. Franz Dykestra and the H. A. Brassert Co. who supplied many chemically analyzed siderite-ankerite ore specimens.

II. EXPERIMENTAL PROCEDURE

The differential thermal analysis equipment used in this study is described in two papers (Kerr and Kulp, 1948; Kulp and Kerr, 1949). The 1948 paper includes a discussion of the theoretical heat relationships.

The ground sample (80–220 mesh) is packed into a cylindrical well which contains one terminal of a two-headed thermocouple. The other terminal is placed in some material, such as alundum, which does not undergo exothermic or endothermic reactions through the heating range. The temperature of the system is then raised at a uniform rate from room temperature to 1050° C. Any thermal changes in the sample well will result in a differential temperature between the two terminals. This is measured by a recording potentiometer in a plot of time or system temperature against differential temperature. The area under a peak on such a curve is proportional to the heat of reaction and concentration of the active ingredients.

In order to make the curve from successive runs and in different wells comparable, the system is calibrated for sensitivity by taking thermal curves of standard kaolinite in each well every few runs. Further, all curves in this study were run in duplicate.

In addition to the DTA curves for all specimens, many of the more interesting or typical specimens were subjected to *x*-ray diffraction for purposes of phase identification. The high and low indices were determined to ± 0.005 for a large fraction of the specimens to check trends in the optical properties with composition and thermal behaviour.

Some chemical data were available for most of the specimens. Eleven of the more typical samples from the Columbia University Mineralogy Collection were analyzed for the common cations and carbon dioxide by Ledoux and Co., New York. H. A. Brassert and Co. supplied complete chemical analyses on nine specimens and partial analyses on thirty two others. In order to interpret the thermal curves of the other specimens they were quickly analyzed for Ca, Fe and Mg by a semi-micro scheme in which known control samples were used. This effectively raised a qualitative method to a semi-quantitative method. The concentration of the three cations in the cation position could be estimated by this method to about $\pm 10\%$.

III. EFFECTS OF PARTICLE SIZE AND DILUENT

It has been shown by many workers that the peak temperature is affected both by the particle and crystallite size as well as the concentration. In the carbonate minerals these effects are particularly marked due to the large peaks, the wide range in particle size in natural occurrences, and the asymmetry of the peaks. In order to interpret the thermal curves of natural carbonate aggregates, it is necessary to have some notion of the amount of temperature shift. These have been established for most of the minerals discussed in this paper but it will suffice for illustrative purposes to discuss only calcite. The paper by Rowland and Jonas (1949) shows the effects for siderite.

Figure 1 shows the particle size effect with calcite. A specimen of Iceland spar from Santa Fe, New Mexico, was crushed and separated into size groups from 50 to 200 mesh. Some of the 200 mesh material was further ground in an agate mortar until the powder was extremely fine (*x*-ray size). In order to obtain the curve of very fine calcium carbonate, some was freshly precipitated from a calcium nitrate solution at room temperature. It appears that the particle size does not affect the curve appreciably down to 200 mesh. For the very fine carbonate particles the temperature is shifted downward. Sedimentary carbonate is usually fine grained but hydrothermal-metamorphic carbonate is more

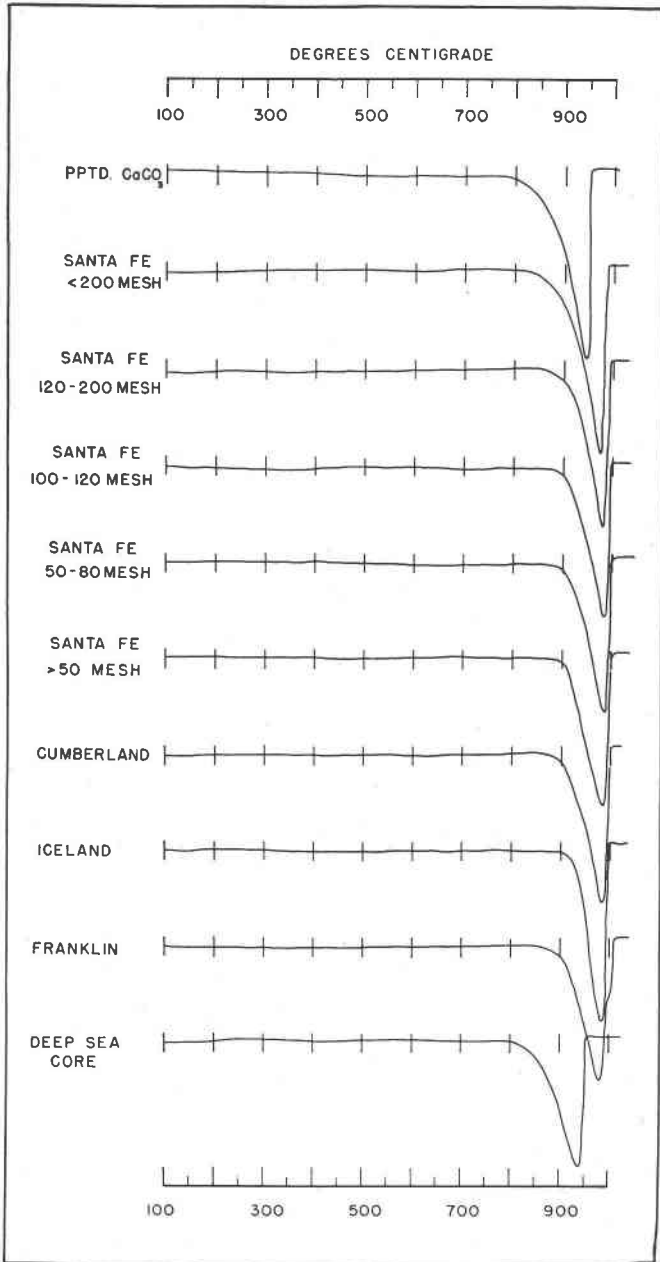


FIG. 1. DTA curves of various specimens of calcite and of various particle sizes for the Santa Fe-Iceland spar.

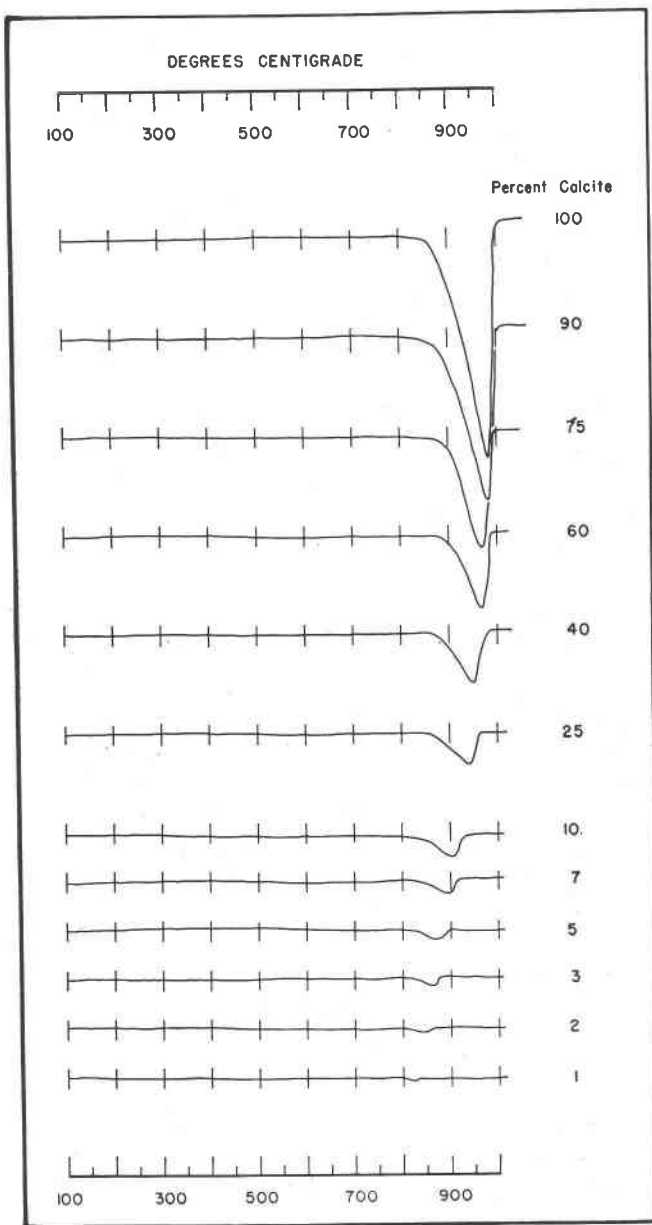


FIG. 2. DTA curves of calcite-alundum mixtures. The calcite is Iceland spar ground to 120-200 mesh.

likely to be rather coarse in texture. It appears that both the peak temperature and the initial decomposition temperature decrease with particle size. The peak temperatures may drop from 980°C to 930°C due to this effect. It is interesting to note, however, that the asymmetry of the curve is not disturbed by a shift in peak temperature. It can be safely assumed that the other carbonates show similar particle size effects. The Cumberland, Iceland, and Franklin calcite specimens are all coarsely crystalline. Only in the case of those carbonates which contain oxidizable ions must this simple picture be modified. In this case the decrease in initial decomposition temperature with particle size follows that of calcite, but the peak temperature may be modified by the ease of oxidation and hence the start of the exothermic reaction.

Figure 2 shows curves of Iceland spar ground to 120–200 mesh and mixed with alundum. The curves show the effects resulting from an inert impurity. The peak temperature is decreased from 980°C to 820°C . The shape of the curve changes considerably, but the initial decomposition temperature does not vary greatly until rather low concentrations are reached. Since this set of curves was obtained with the

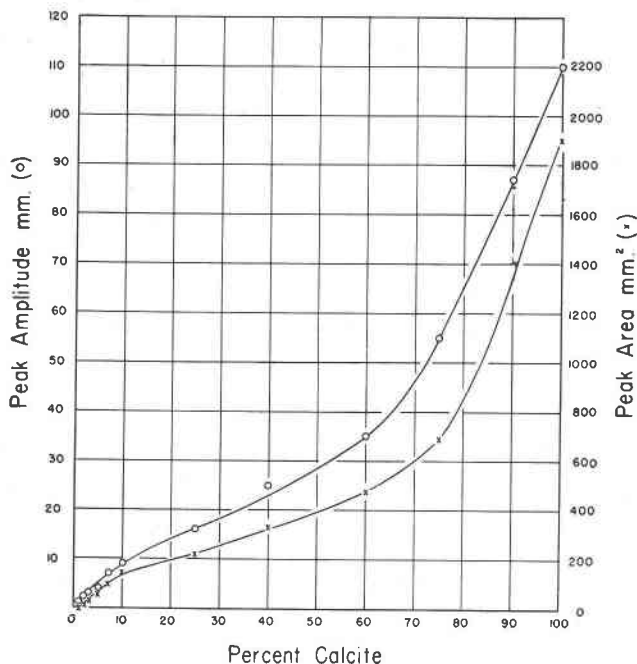


FIG. 2a. Peak area and amplitude against concentration for coarse calcite-alundum mixtures.

coarse calcite, it would seem that the combination of very fine particle size and low concentration might produce calcite peaks as low as 800° C. The characteristic asymmetry of the calcite peak assists in identifying the mineral in low concentrations.

Figure 2a shows the data of Fig. 2 plotted for use as a calibration curve for quantitative estimation. It is apparent that either peak area or peak amplitude may be used as a concentration index providing conditions are equivalent in the calibration sample and the unknown. However, the area remains relatively constant with changing particle size while the amplitude varies; hence the area is to be preferred practically. Theoretical considerations (Kerr and Kulp, 1948) agree that this should be the case.

IV. DTA OF CA-MG-FE CARBONATE MINERALS

The minerals studied include calcite, siderite, magnesite, dolomite, ankerite, and natural mixtures of these. Figure 3 shows the "ideal" DTA curves for these minerals as obtained from this study. For these "ideal" curves it is assumed that the samples are coarsely crystalline, chemically pure and have been run in a thermal analysis unit of the type described by Kerr and Kulp (1948). The shapes of the oxidation peaks are not as readily reproducible even with a fixed experimental arrangement as the other peaks.

A. Calcite

The general features of the DTA curves of calcium carbonate have been suggested by several workers, but Faust (1950) was the first to publish a detailed study of the thermal properties of aragonite and calcite. DTA curves of calcite from various localities have been included in this report to complete the group. Figure 1 shows the curves of five calcite specimens. Clear coarse calcite from Iceland gives the sharpest peak. The sample from Franklin may be a mixture of two calcites of different crystallite size. Faust (1950) observed subsidiary breaks on the high temperature side of the peak in samples which were mixtures of calcite and aragonite. This was attributed to different decomposition temperatures for the primary calcite and the calcite produced from the aragonite transformation at 400–450° C. Since the peak characteristic of this transformation does not appear in the thermal curve of the Franklin sample, it is likely that two calcites are present rather than a mixture of aragonite and calcite. An x-ray pattern of this sample confirmed the absence of aragonite.

All calcite curves show an elevation of the base line after the decomposition due to the difference in specific heat of calcite and CaO. The

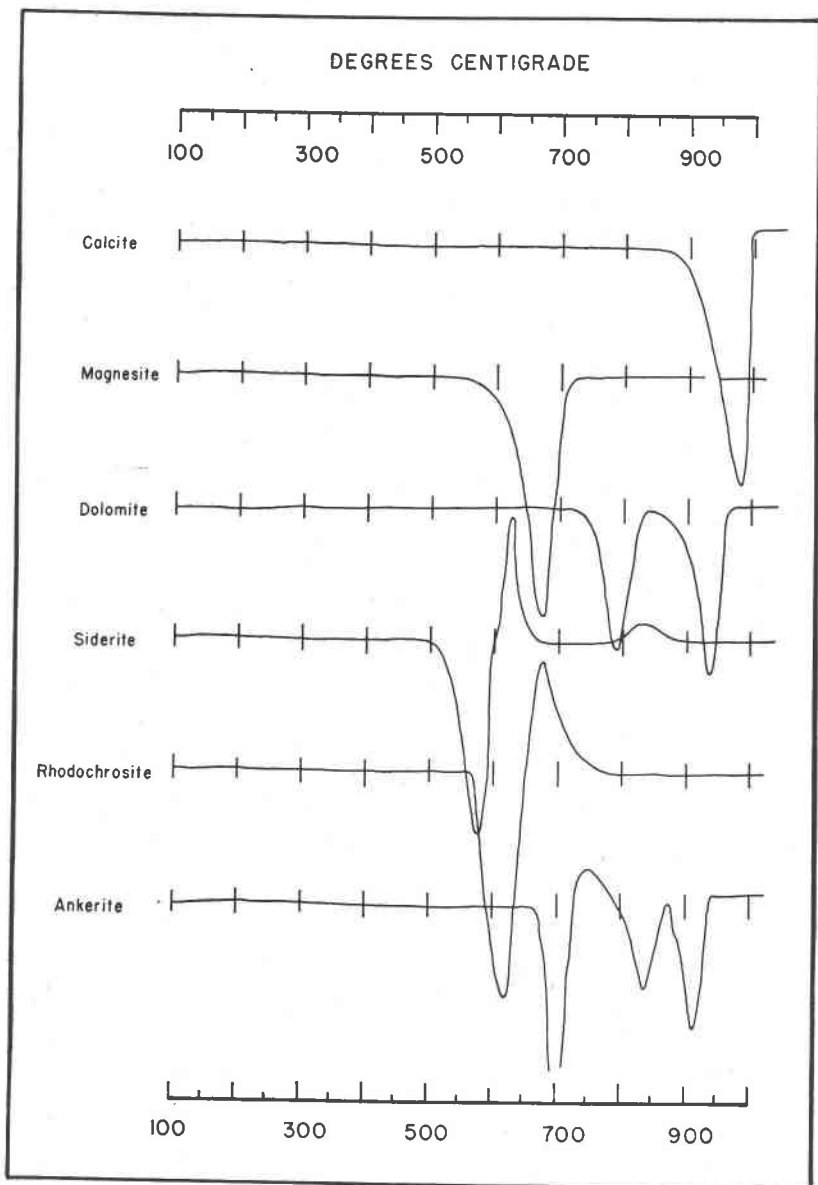


FIG. 3. Theoretical DTA curves for pure carbonate mineral mixtures.

deep sea calcite taken from an Eocene core in the North Atlantic shows a lower peak temperature as expected for the very fine particle size. The broad peaks sometimes observed on natural calcite aggregates indicate a wide spread of particle size.

B. Siderite

There are a number of published DTA curves of siderite (Cuthbert and Rowland, 1947) (Kerr and Kulp, 1947) and (Fredrickson, 1948). Rowland and Jonas (1949) have contributed considerably to the knowledge of the thermal behaviour of siderite. They were particularly concerned with the interpretation of the variation in the peaks due to rates of oxidation.

If a specimen of siderite of the ideal composition is thermally analyzed in air without dilution by an inert substance, a curve such as that shown in Figure 3 will result. The exact shape of the exothermic peak will be dependent on the tightness of packing, size and shape of the sample well, and particle size. The endothermic peak represents the decomposition of siderite to FeO. This is oxidized to Fe_2O_3 giving the major exothermic peak. The product after the first exothermic peak is a mixture of hematite ($\alpha\text{-Fe}_2\text{O}_3$) and maghemite ($\gamma\text{-Fe}_2\text{O}_3$). The proportion of these polymorphs is determined by the rate of oxidation and the degree of substitution in the siderite lattice. Apparently oxygen catalyzes the transformation to $\alpha\text{-Fe}_2\text{O}_3$ for the more open sample, the more $\alpha\text{-Fe}_2\text{O}_3$ formed. This is to be expected since maghemite is essentially a spinel lattice with defects. Apparently magnetite does not form under these conditions. The second exothermic peak is due to the transformation of $\gamma\text{-Fe}_2\text{O}_3$ to $\alpha\text{-Fe}_2\text{O}_3$. The material at 1000°C is essentially hematite. X-ray patterns of samples, which were heated to various temperatures in this work, confirm the data and interpretation of Rowland and Jonas (1949). Beck (1950) failed to mention the second endothermic peak and its significance even though it is apparent in the thermal curve of a specimen labelled "Saxony."

Figures 4 and 5 show the DTA curves of some representative siderite specimens which permit a number of general conclusions to be drawn. If the specimen is so coarsely crystalline that all of the crystal grains are larger than the ultimate mesh size after crushing, a sharp peak such as that obtained in 4-10, 5-6, or 5-11 is obtained. A relatively broad endothermic peak such as 4-8 or 5-1 is indicative of a wide range in crystallite size. The initial decomposition temperature, which in these curves ranges from 5-1 (380°C) to 4-12 (600°C), is dependent on both crystallite size and substitution of Mn^{++} and Mg^{++} for Fe^{++} . A gradual deviation from the base line such as 4-8 or 5-1 compared to a sharp break as in 4-10

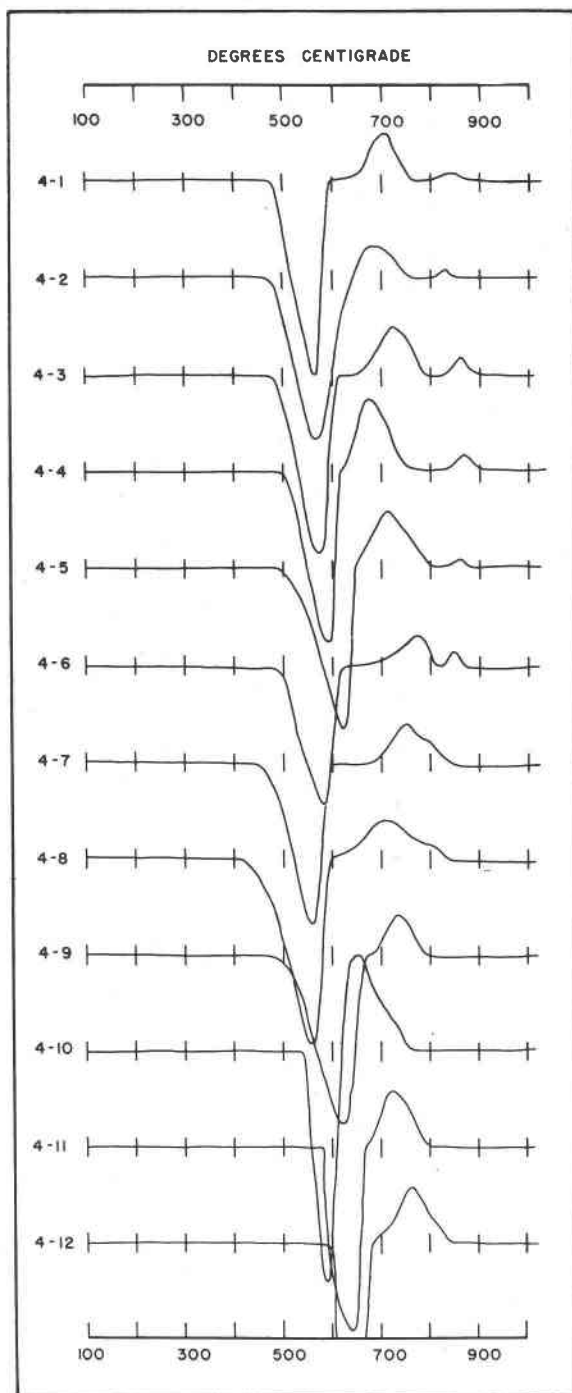


FIG. 4. DTA curves of selected siderite specimens:

- 4-1 Waldstein, Carinthia
- 4-2 Roxbury, Conn. (1)
- 4-3 Andreasburg, England
- 4-4 Roxbury, Conn. (2)
- 4-5 Porco, Bolivia
- 4-6 Pöbraz, Bohemia
- 4-7 Devonshire, England
- 4-8 Cornwall, England
- 4-9 Dauphine, France
- 4-10 Neudorf, Germany
- 4-11 Traversella (1), Italy
- 4-12 Germany

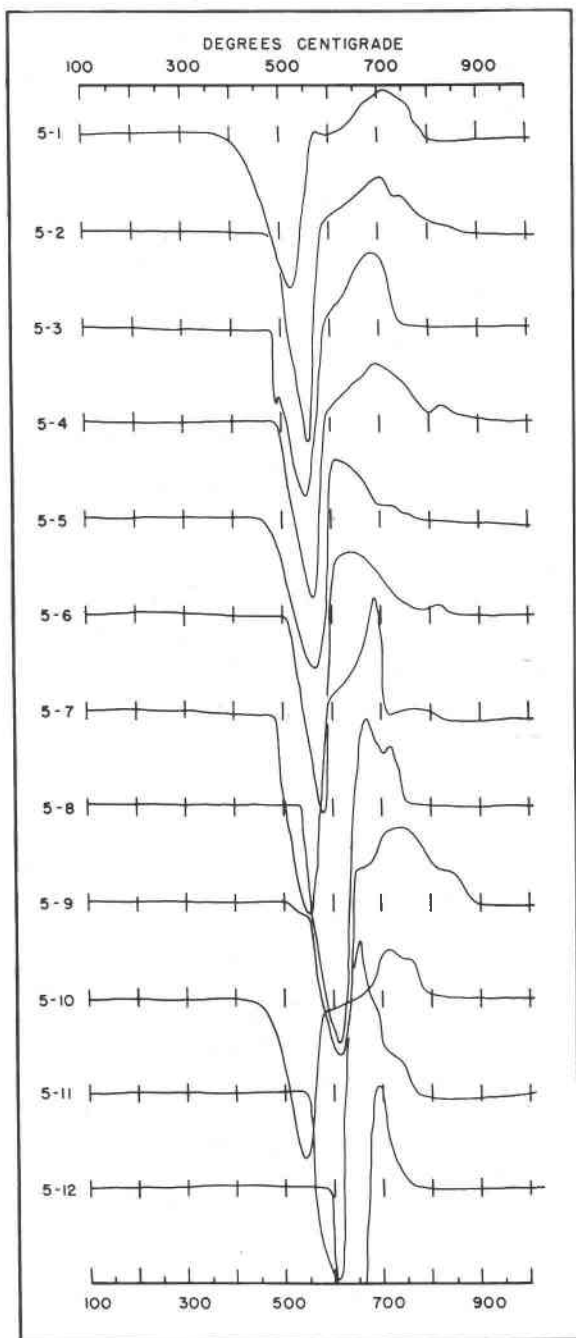


FIG. 5. DTA curves of selected siderite specimens:

- 5- 1 Redrush, Cornwall (1)
- 5- 2 REO 6A (Styria)
- 5- 3 Danville, Pa.
- 5- 4 KLE 2B (Styria)
- 5- 5 Crassbackel (Styria)
- 5- 6 KLE 2A (Styria)
- 5- 7 Westphalia, Germany
- 5- 8 Mines de Allerd, France
- 5- 9 Galpina Co., Calif.
- 5-10 Missouri
- 5-11 Rutland, Vt.
- 5-12 Brazil (2)

or 4-11 indicates a range in particle size. In the latter case, particle size is probably quite important in determining the peak temperature.

Most natural siderite specimens contain a few per cent MnO. Usually this is not enough to shift the peak temperature since even pure rhodochrosite has an endothermic peak temperature of only 620–630° C (Kulp, Wright and Holmes, 1949). The average endothermic peak temperature for reasonably pure coarse siderite is near 550° C. Beck (1950) shows a DTA curve of a siderite with 17% MnCO₃ with the endothermic peak near 580° C. Samples 5-2, 5-4, and 5-6 had only 2% MnO present so the higher temp. of 5-6 must be attributed to Mg or Ca substitution. Semi-quantitative analysis shows 5-6 to contain considerable Mg (20 ± 5% cation positions) but insignificant Ca. That the Mg is more important than Mn in raising the peak temperature is expected since the decomposition temp. of magnesite is 700° C. Chemical analysis of the Roxbury sample (4-4) which gave a peak at 570° C was 4.10% MgO while the Dauphine specimen (4-9) gave a peak at 600° C and contained 13.07% MgO. While quantitative chemical analyses were not available for the other samples, semi-quantitative analysis showed that all the specimens with high peak temperature such as 4-5, 4-10, 4-11, 4-12, 5-8, 5-9, 5-11, 5-12 to be high in magnesium, while 4-1, 4-2, 4-7, 4-8, 5-1, 5-2, 5-3, 5-4, 5-5, 5-7, and 5-10 were low in MgO content.

The areas under the endothermic peaks vary more in the case of siderite than calcite because the exothermic reaction is so intimately tied to the endothermic reaction. For careful quantitative work with siderite in natural aggregates, it is necessary to work in an inert atmosphere so that the readily reproducible endothermic peak could be studied alone.

The variations in the exothermic peaks require further study but some features may be defined. The second exothermic peak appears to vary both in peak temperature and amplitude. Since the concentration and distribution of γ -Fe₂O₃ depends on the rate of oxidation, the extent of substitution and the presence of impurities, it is expected that neither the concentration of γ -Fe₂O₃ nor the temperature of transformation of γ -Fe₂O₃ to α -Fe₂O₃ is constant. For the most typical siderite specimens in which substitution is unimportant, the second exothermic peak appears between 830 and 860° C as in 4-1, 4-2, 4-3, 4-4, 4-5, 4-6, 5-4, and 5-6. Occasionally this peak may occur at a lower temperature and may be blended into the first endothermic peak, particularly if the latter is delayed in its appearance. Such a relationship is suggested in curves 4-7, 4-8, 4-10, 5-1, 5-2, 5-5, 5-7, 5-9, 5-10, 5-11. All specimens in which the decomposition starts at 500° C or less show the two exothermic peaks. However, in the samples with the highest Mg content (4-9, 4-11, 4-12, and 5-12), which have endothermic peak temperatures in excess

of 600° C, the second exothermic peak appears insignificant. With high Mg content, therefore, the products are probably hematite and periclase. While it is possible that magnesioferrite ($\text{MgO} \cdot \text{Fe}_2\text{O}_3$) could form under these conditions, the evidence for its existence from *x*-ray diffraction patterns taken on material heated to 1000° C is inconclusive. In general the area under the exothermic peaks decreases with increased magnesium substitution. Compare, for example, 4-9 with 4-10. The low area and delayed peak temperature for 4-6 is due to the presence of clay material which prevented ready access of the air to the FeO.

The optical and *x*-ray data for these specimens of siderite proved consistent with the DTA curves and the chemical composition. On all samples with little substitution, the low index was 1.63 to 1.65 and the high index 1.86 to 1.88. The samples with 20% Mg in the cation positions gave a low index of 1.59 to 1.60 and a high index of 1.80 to 1.82. The indices for pure magnesite are low 1.52 and high 1.70. The data do not justify a plot since the index is affected by Ca and Mn substitution as well as Mg. An analogous relationship held for the "d" values calculated from powder patterns.

C. Magnesite

The DTA of several magnesite curves has been reported in the literature. They are not all consistent. Faust (1949) shows a thermal curve of a magnesite listed as pure which shows an exothermic peak following the main endothermic peak. This is probably due to iron substitution in the lattice. Pure coarsely crystalline magnesite yields a simple endothermic peak at about 680–700° C. The reaction product is periclase, identified by *x*-ray diffraction.

Figure 6 shows the thermal curves of the selected magnesite specimens. The effect of particle size is present but to a less extent than in calcite. Specimens 6-8, 6-9, and 6-10 are visibly grained whereas the other specimens were microcrystalline. The initial decomposition temperature and the peak temperature are related to particle size. Chemical analysis of 6-1 shows 1.57% CaO and 1.14% Fe_2O_3 with 46.12% MgO. If the calcium is present as calcite, even this small amount should show on the thermal curve (See Fig. 2). The quantity of iron is apparently insufficient to produce a visible exothermic reaction. Both Ca and Fe are therefore presumably substituted and roughly balance each other in effect on the peak temperature. It is thought that 6-1 is nearly representative of the ideal curve for magnesite. Semi-quantitative chemical analysis and optical examination indicate that 6-2 is quite similar to 6-1. The thermal curve indicates a slightly higher CaO concentration. 6-3 has less iron than 6-1 (semi-quantitative) but has 1–2% Ca. The DTA curve indi-

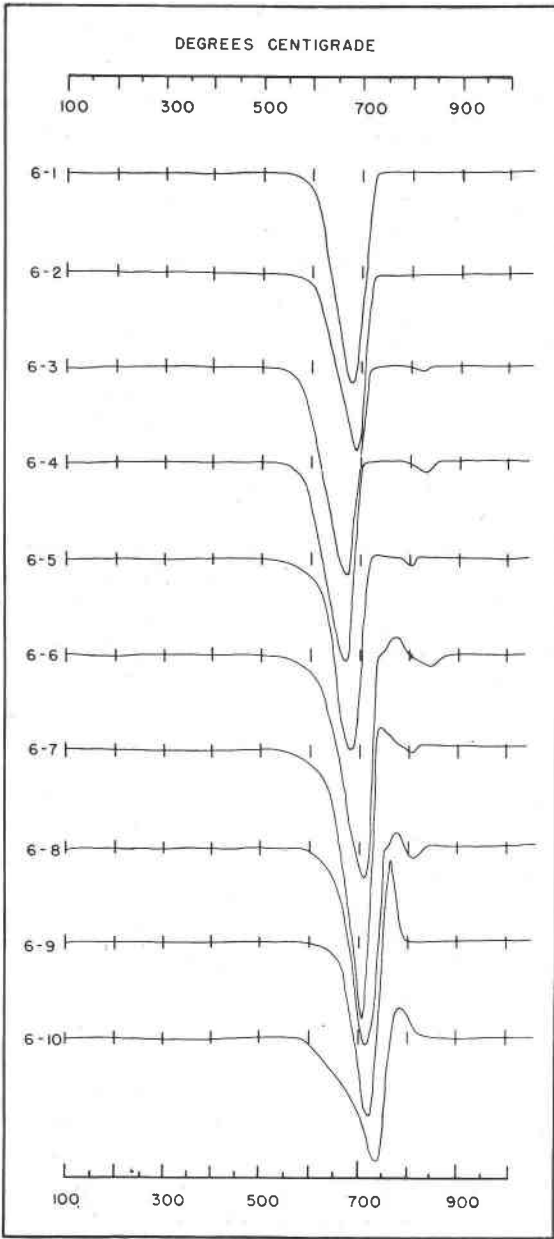


FIG. 6. DTA curves of representative magnesite specimens:

- 6- 1 Moravia, Czech.
- 6- 2 Baumgarten, Germany
- 6- 3 Halilona
- 6- 4 Brucite, Nevada
- 6- 5 Muntodi
- 6- 6 Hoboken, N. J.
- 6- 7 Eureka, Nevada
- 6- 8 Trieben
- 6- 9 Greiner, Austria
- 6-10 Chewelah, Wash.

cates this is present as calcite (820° C peak). 6-4 and 6-5 are very similar to 6-3 but with slightly higher CaO content. In 6-5 it appears that some of the Ca is in the magnesite lattice due to the higher peak temperature despite the low initial decomposition temperature. 6-6 has more iron and calcium (est. 1-5% each) than 6-5. The substituted iron is sufficient to produce an exothermic peak and the calcium is distributed between substituted calcium and calcite (est. 5%). 6-7 is similar to 6-6 in composition but apparently the admixed calcite is of finer crystallite size. 6-8 from Trieben showed 2.00% CaO and 2.20% Fe₂O₃ on analysis. It appears that roughly half of the calcium is present as calcite and half in the lattice. The higher peak temp. is related primarily to the particle size. The sample from Greiner (6-9) gave an analysis: CaO, 0.79%; Fe₂O₃, 11.37%. It was the coarsest magnesite studied. The peak size and shape is consistent with this physical and chemical data. 6-10 has a fairly coarse texture, is estimated to have 5% Fe₂O₃ and may contain some inert impurities. The extreme asymmetry of the curve may indicate a mixture of siderite and magnesite, or two magnesites in which one generation contains most of the iron.

In general the optical data show both indices to be higher for the specimens containing more iron. Since these samples have three or four cation components (Ca, Fe, Mg, Mn), the optical data do not fall on a smooth curve from magnesite to siderite. They may be used, however, to indicate iron substitution providing the calcium content is not too high. The *x*-ray "d" values show the same trends.

D. Dolomite-Ankerite

It is reasonable to treat these minerals under one section because they are structurally identical and continuously related. "Dolomite" with less than 1% Fe₂O₃ is rare and "ankerite" with a simple Mg:Fe ratio of 1:1 is uncommon. Ankerites have been found in this study in which the iron in the magnesium positions ranges from 5% to 70%.

Faust (1949) has published a curve for dolomite and Beck (1950) shows the curves of one dolomite and two ankerites. However, little has been recorded about the thermal-structural relationships of this important group of carbonates.

The structure of dolomite (Bragg 1937) does not consist of randomly substituted Mg ions in a calcite lattice but rather has two distinct cation positions, the smaller occupied by the Mg and the larger by the Ca. The two cations alternate in layers perpendicular to the *c*-axis. While examples of magnesian calcite have been cited, generally there is a distinct break between dolomite and calcite. The dolomite lattice provides a more stable way to pack equal quantities of Ca and Mg among carbonate

ions. From this picture of the lattice one would assume that the Fe ions would substitute primarily in the Mg positions. Actually this is found to be amazingly rigorous in the following data.

Figures 7 and 8 show the thermal curves of some representative dolomite-ankerite specimens. It is evident that dolomite, when sufficiently pure, such as 7-1, 7-2, and 7-3 yields two endothermic peaks while ankerite displays three. The peak shapes, amplitudes and positions depend on the crystallite size, degree of substitution, and the amount of mixing of different minerals of this group.

The first endothermic peak in either dolomite or ankerite is due to the decomposition of the carbonate ions most closely associated with the magnesium positions. The temperature at which this peak occurs depends on the particle size and iron substitution. The temperature at which the decomposition initiates is also determined by these factors. The sharpness of this peak is related to grain size primarily so this can be used to delineate the effects of particle size and substitution on the peak temperature. X-ray patterns of ankerites heated past the first endothermic peak are diffuse but indicate the presence of calcite, MgO and maghemite as separate phases even though they must be separated on a very fine scale. This fails to agree with Beck (1950) who stated that the first peak is due to the decomposition of iron carbonate only. No dolomite lines have been found in any of these specimens after heating past the first peak. Further, the size of the second endothermic peak increases continuously with increasing Fe^{++} content. Therefore, it can not be due to $MgCO_3$ decomposition as Beck suggests.

The second endothermic peak in dolomite (7-1) and the third peak in ankerite remain fairly constant in temperature, shape and amplitude. Both are broadened and reduced in amplitude and temperature by inert impurities (8-9), and are somewhat affected by total iron content. This peak is due to the release of CO_2 attached to the calcium ions.

The middle endothermic peak in ankerite has several interesting features. It increases in area with increase in iron concentration in Mg positions. Further, temperature of the peak is essentially independent of particle size or substitution.

The exothermic oxidation of Fe^{++} to Fe^{+++} after the initial decomposition is generally masked but in those samples of high iron content such as 7-8 and 7-10, the exothermic reaction is quite distinct.

Quantitative chemical analyses are available for a number of the specimens used in obtaining Figure 7. The other specimens in Figs. 7 and 8 were either partially analyzed quantitatively or semi-quantitatively. An evaluation of the thermal data in terms of these analyses is instructive. Table 1 shows the quantitative chemical data recomputed on a

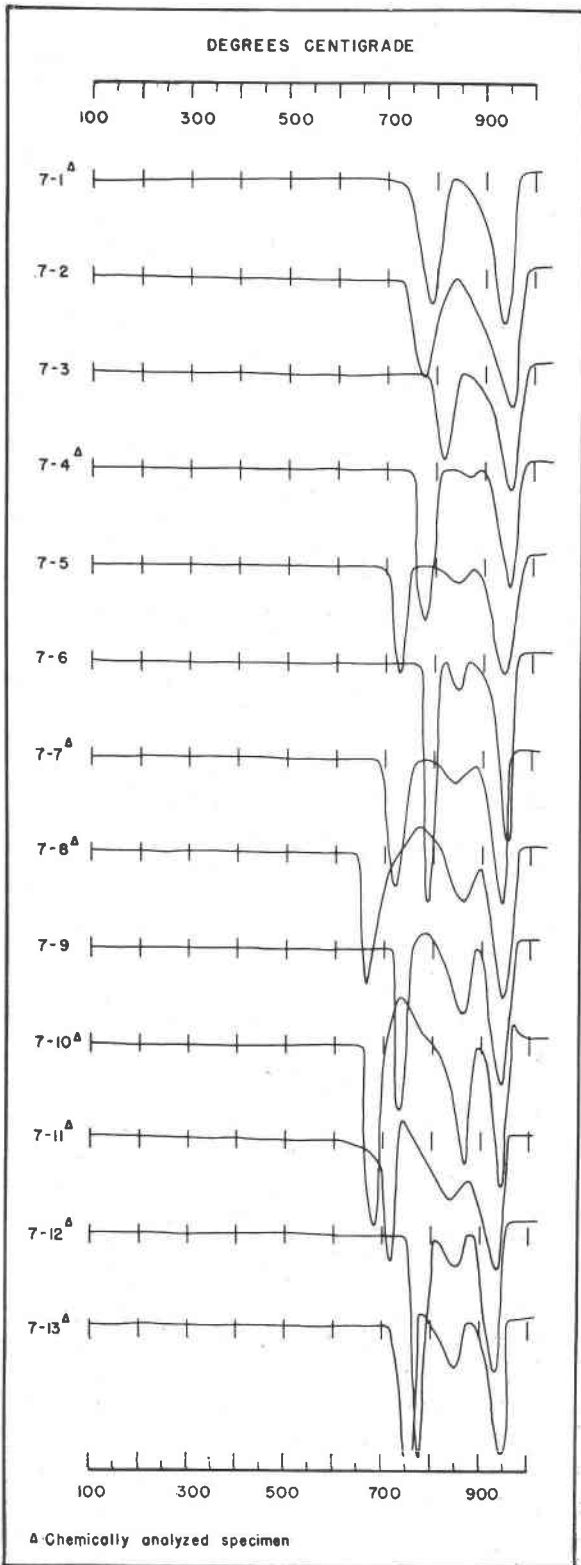


FIG. 7. DTA curves of selected dolomite and ankerite specimens:

- 7- 1 Oberdorf, Styria
- 7- 2 New Almaden, Calif.
- 7- 3 Traversella (2) Italy
- 7- 4 Chamouni, France
- 7- 5 Ishanimland
- 7- 6 Isle of Man, England
- 7- 7 Freiberg, Saxony
- 7- 8 Redrush, Cornwall (2)
- 7- 9 Phoenixville, Pa.
- 7-10 Mouzaia, Algeria
- 7-11 Ro Reich 23A (Styria)
- 7-12 Ro Arm 28A (Styria)
- 7-13 Ro Arm 27A (Styria)

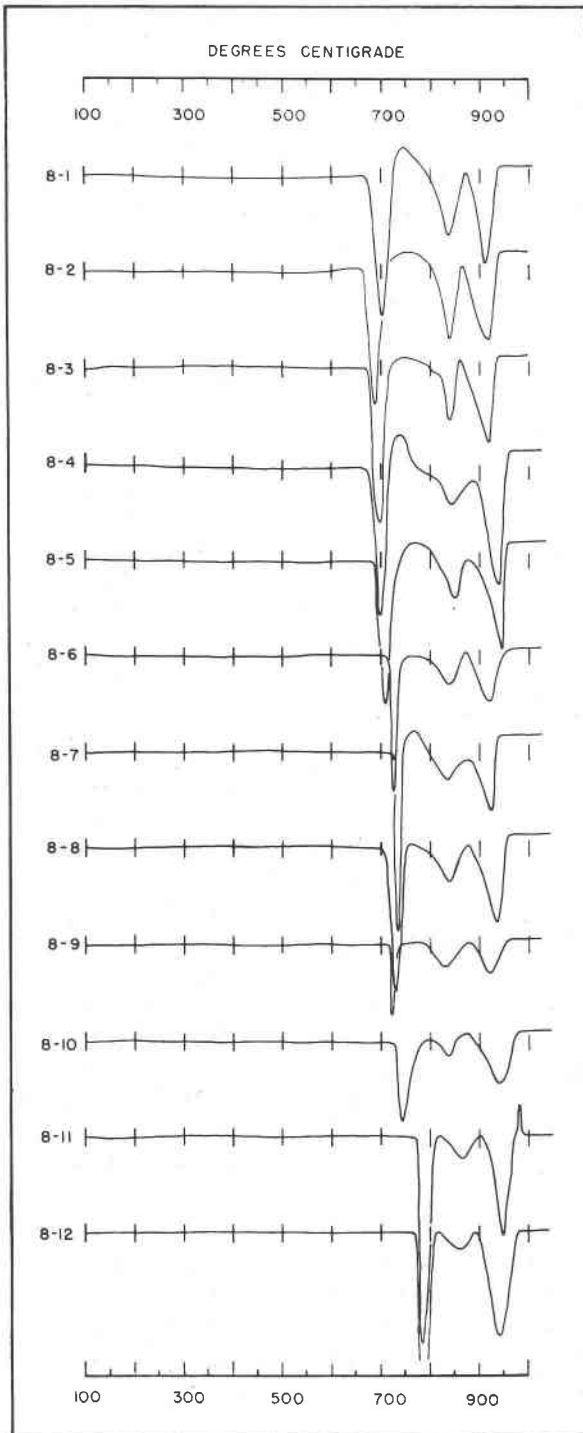


FIG. 8. DTA curves of selected ankerite specimens:

- 8- 1 Eitzterge, Styria
- 8- 2 Eisenertz, Styria
- 8- 3 Admont, Styria
- 8- 4 Gassite, Germany
- 8- 5 Ro Reich 21A (Styria)
- 8- 6 Ro Reich 24B (Styria)
- 8- 7 AEU 18A (Styria)
- 8- 8 OAM 9B (Styria)
- 8- 9 Ro Reich 22A (Styria)
- 8-10 Ro Arm 26A (Styria)
- 8-11 Brazil (1)
- 8-12 Brazil (5)

molar basis for each ion, assuming 4 moles of CO_2 . These specimens were essentially free from insoluble residues but where residues were present the sample was corrected for this effect. In these computations the manganese oxide which is present in quantities up to 2%, is included in the figure for iron. Whatever assumption is made regarding Mn the conclusions are not affected.

TABLE 1

Locality	Run No.	Moles Mg^{++}	Moles Fe^{++}	Moles Fe^{++} + Mg^{++}	Moles Ca^{++}
Oberdorf	7-1	1.94	0.07	2.01	2.00
Chaumoni	7-4	1.68	0.40	2.08	2.00
Freiberg	7-7	1.33	0.70	2.03	2.01
Redrush	7-8	0.93	1.05	1.98	1.95
Mouzaia	7-10	0.82	1.16	1.98	2.03
Styria 23A	7-11	0.82	1.10	1.92	1.99
Styria 28A	7-12	1.35	0.66	2.01	1.98
Styria 27A	7-13	1.02	0.88	1.90	2.04
Tri State (Beck)		1.07	0.74	1.83	2.10
Theo. dolomite		2.00	0.00	2.00	2.00
Theo. ankerite		1.00	1.00	2.00	2.00

The most striking thing about these data is the clear proof that substitution of Fe^{++} takes place exclusively in the Mg positions such that the *sum* of the moles of Fe^{++} and Mg^{++} is equal to the moles of Ca present. The consistent area under the last endothermic peak in dolomite and ankerite would be expected from these data. It will also be observed that the purest white dolomite (Oberdorf, 7-1) contains iron and that there are no apparent discontinuities in the Mg-Fe substitutions. The specimen from Redrush, Cornwall (7-8) appears to be a typical ankerite. Semi-quantitative tests show 7-4 and 7-6 to be low in iron while 7-5 and 7-9 are considerably higher.

The significance of the peaks may be interpreted with the help of *x*-ray powder patterns. The first peak is due to the decomposition of the magnesium positions in the lattice. This also releases the iron which becomes oxidized to Fe_2O_3 .

It might be expected that the second endothermic peak is due to the formation of $\text{MgO} \cdot \text{Fe}_2\text{O}_3$. This does not appear to be the case. Rather the second endothermic peak seems due to the formation of the compound $\text{Fe}_2\text{O}_3 \cdot \text{CaCO}_3$. A mixture of finely ground hematite and calcite in a 1:1 ratio produced the same peak as observed in these ankerite specimens. Finally after heating to 1000° C the *x*-ray patterns obtained from these

specimens failed to contain lines of CaO and $\text{MgO} \cdot \text{Fe}_2\text{O}_3$ as Beck claimed for his samples, but rather strong lines of calcium ferrite $\text{CaO} \cdot \text{Fe}_2\text{O}_3$ and MgO (diffuse). Although there is a considerable heat of reaction in the formation of $\text{Fe}_2\text{O}_3 \cdot \text{CaCO}_3$, it apparently does not greatly affect the heat required to liberate the carbon dioxide from the calcium ions since the last endothermic peak does not appear too greatly affected by iron content. There is some indication that the formation of this compound reduces the heat of decomposition for the residual carbonate ions.

Figure 9 shows the peak temperature of the first endothermic reaction and the area of the second endothermic peak plotted against iron con-

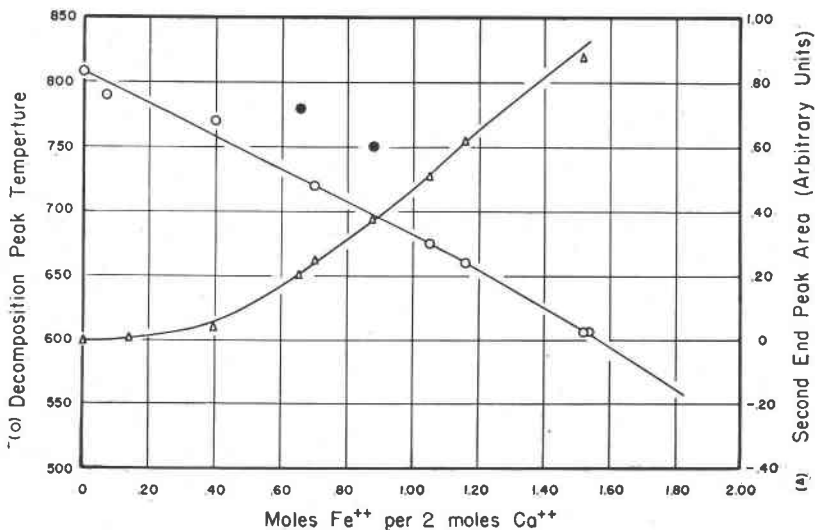


FIG. 9. Moles of substituted Fe^{++} versus decomposition peak temperature (left ordinate) and second endothermic peak area (right ordinate).

tent. The points fall on a smooth curve except for the two unusually coarse grained samples indicated as solid circles. A great difference in crystallite size will appear in a higher decomposition temperature. Once the lattice is destroyed, however, the initial grain size is not very significant hence the values of the second endothermic peak area for these same two samples fall in line. Sample 7-11, which is also quite coarse, is omitted from this figure because of the unusual overlapping of the exothermic peak on the second endothermic peak thus making it difficult to choose an accurate value for the peak area of the second endothermic reaction. It is important to observe that the second endothermic peak area against moles of Fe continues to rise after 1.00 moles of FeO has been reached. This is consistent with the formation of a 1:1 compound $\text{Fe}_2\text{O}_3 \cdot \text{CaCO}_3$.

If a spinel-like compound were forming between $\text{Fe}_2\text{O}_3 \cdot \text{MgO}$ then the heat of this reaction should go through a maximum at FeO 1.00 moles.

Figure 8 shows the thermal curves of a number of specimens of ankerite. The relative sensitivity between these curves and those in Fig. 7 may be compared by equating the CaCO_3 decomposition peak of 7-9 and 8-1. The first five ankerites 8-1 through 8-5 are high in iron content. Thus decomposition peaks as low as 590°C are obtained and the second endothermic peak is correspondingly high. Sample 8-5 has a total Fe analysis of 23.1% as compared to 13.4% for 7-13. This indicates about 1.53 moles of FeO . Curves 8-6 and 8-7 show less than the first five samples but about 1.00 moles of Fe. Note the unusually homogeneous crystalline size as displayed by the extremely sharp decomposition peaks. 10–20% hematite, or other inert impurity, is indicated by the maximum peak height of the CaCO_3 decomposition. 8-8 has less foreign constituent and has a wider range in crystallite size. 8-9 and 8-10 are both diluted with thermally inert constituents—mostly hematite but show a considerable difference in iron substitution in the ankerite. 8-11 and 8-12 are similar except for the exothermic peak at 990°C in 8-11. This was also observed on the Mouzaia sample (7-10). It is attributed to the conversion of $\gamma\text{-Fe}_2\text{O}_3$ to hematite. Why it should be so delayed in this particular specimen is not clear. If the iron content became sufficiently high so that there was more $\gamma\text{-Fe}_2\text{O}_3$ than that required to form $\text{Fe}_2\text{O}_3 \cdot \text{CaCO}_3$ this might be expected. The thermal curve of 8-11 does not indicate this much iron. It is possible that this is a case of some minor iron substitution in the calcium positions. This is possible to a minor extent on theoretical grounds.

E. Natural Carbonate Aggregates

Figures 10, 11 and 12 show the DTA curves for a considerable number of natural carbonate mixtures. The interpretation of these curves in terms of the foregoing discussion will illustrate the application of these concepts.

10-1 shows a sample consisting of about 80% siderite, 5–10% ankerite, and 5–10% silicate and inert. The ankerite appears to have a Fe:Mg ratio near 1:1. The chemical analysis shows: CO_2 36.02%, Fe_2O_3 0.46%, FeO 48.09%, MnO 2.67%, CaO 1.59%, MgO 3.19%, SiO_2 6.1%. From the analysis it appears that some of the Mg^{++} is probably substituting in the siderite lattice.

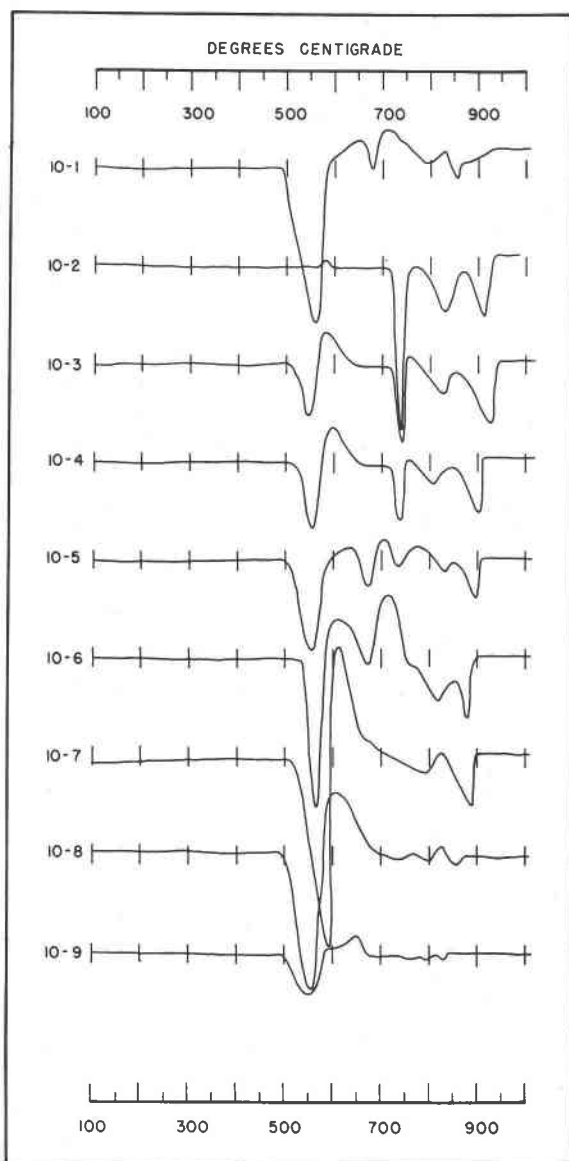


FIG. 10. DTA curves of ankerite-siderite natural aggregates from Erzberg Mine, Styria, Austria:

- 10- 1 KLE 1A
- 10- 2 AEO 10B
- 10- 3 AEU 18B
- 10- 4 AEU 20A
- 10- 5 REO 6C
- 10- 6 REO 6B
- 10- 7 REO 6B-2
- 10- 8 REO 7A
- 10- 9 REU 15C

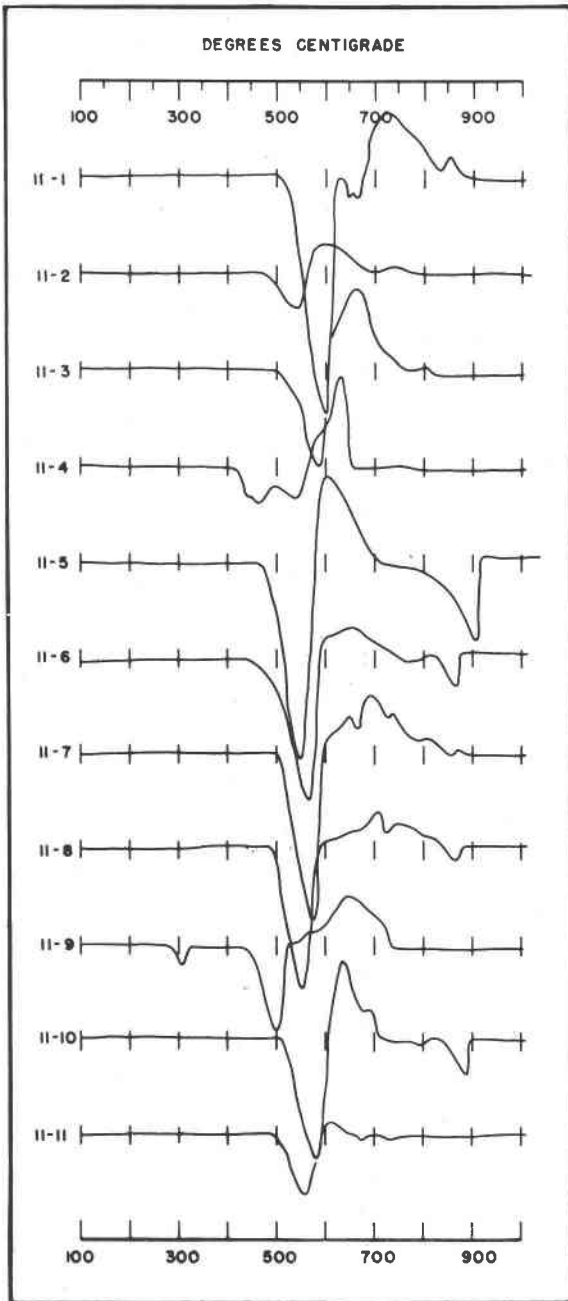


FIG. 11. DTA curves of natural siderite mixtures:

- 11- 1 Lobenstein, Germany
- 11- 2 Nassau
- 11- 3 Cornwall, England
- 11- 4 Maryland
- 11- 5 Batino, Tuscany
- 11- 6 Bear Run, Pa.
- 11- 7 REU 15A (Styria)
- 11- 8 REU 14A (Styria)
- 11- 9 Redrush (fibrous)
- 11-10 REO 7B (Styria)
- 11-11 REO 8A (Styria)

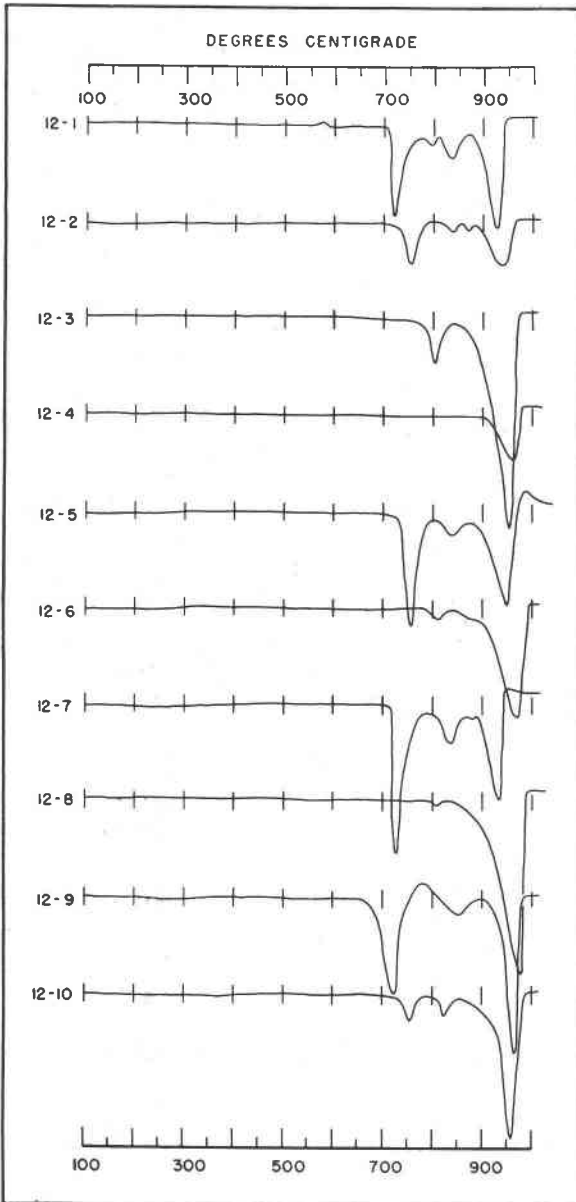


FIG. 12. DTA curves of natural carbonate aggregates:

- 12- 1 AEO 10A (Styria)
- 12- 2 AEO 12A (Styria)
- 12- 3 Ro Reich 21B (Styria)
- 12- 4 OAM 9A (Styria)
- 12- 5 AEO 11A (Styria)
- 12- 6 Ro Reich 24A (Styria)
- 12- 7 AEU 19A (Styria)
- 12- 8 REU 13A (Styria)
- 12- 9 Schemnitz, Hungary
- 12-10 Joplin, Mo.

10-2 shows the reverse of 10-1 with 3-5% siderite and 70% high iron ankerite. This sample contains 22.1% total Fe. With such a low siderite content, this indicates an ankerite with about 1.5 moles of Fe^{++} .

10-3 and 10-4 are quite similar containing about 20-30% siderite and 50-60% ankerite with about 1.00 moles of Fe^{++} . The difference in the areas of the last endothermic peak between 10-2 and 10-3 shows the effect of the greater iron content of 10-2 on the $\text{Fe}_2\text{O}_3 \cdot \text{CaCO}_3$ decomposition.

10-5 is a most interesting specimen showing three carbonate minerals present: siderite 50%, magnesite 20% and ankerite 30% with about 1.0 moles of Fe^{++} .

10-6 appears to contain 60% siderite, 20% magnesite and 20% dolomite. 10-7 shows about 80% siderite containing some magnesium substitution with about 20% dolomite (or 10% dolomite and 10% calcite). Magnesite seems absent in this specimen although the $\gamma\text{-Fe}_2\text{O}_3$ transformation to hematite is detectable near 680° C. 10-8 contains about 60-70% of rather pure siderite with 10% or less dolomite-ankerite. This specimen analyzed 5.32% CaO and 4.01% MgO. The x-ray pattern shows only siderite lines. 10-9 shows about 20% siderite and 5% ankerite. The major impurity in 10-9 is hematite. The specimen analyzed 38.5% total Fe.

11-1 appears to be a high grade siderite except for the little doublet between 600 and 700° C. This appears to be due to two differently substituted magnesites. 11-2 simply contains 20% siderite with inert material. 11-3 may contain two siderites which add up to about 40%. 11-4 contains sulfides and siderite. The dominance of the exothermic peak over the endothermic peak is due to the rapidity of oxidation. The size of the exothermic peak indicates the presence of 30-50% siderite. The peaks between 400 and 500° C are attributed to the sulfides. 11-5 consists of 80% siderite and 20% fine calcite. 11-6 has 60% siderite and 10% calcite. There is the possibility of a few per cent of dolomite. 11-7 contains 75% siderite with some Ca substitution, 5% magnesite and a few per cent of dolomite. This specimen analyzed 6.93% CaO, 3.14% MgO, and 19.7% insoluble. 11-8 contains 50-6% siderite, 5% calcite and a trace of dolomite. This specimen has a total iron content of 35.20% Fe indicating hematite as an impurity. 11-9 shows 5% goethite (300° C), 40% of a very fine siderite and no other carbonates. 11-10 shows 70% siderite with considerable Mg substitution, 10% calcite and a few per cent dolomite. 11-11 shows an impure siderite (est. 20%). It is mixed with considerable hematite. The total analysis for 11-11 is 41.2% Fe.

12-1 appears to contain 2-3% siderite, 70% ankerite and about 0.8 moles of Fe and 10% dolomite. This specimen analyzed 9.56% MgO

and 23.10% CaO. The FeO was 20.2%. 12-2 is similar to 12-1 but contains no trace of siderite and has nearer to 30% ankerite. The total Fe content of 26.6% indicates some hematite which was observed in the x-ray patterns. 12-3 is a dolomite (20%), calcite (80%) mixture. The total iron content of this specimen was 2.75% which was present largely as a hematite stain. 12-4 is an ironstained calcite (20%). 12-5 is a reasonably low iron ankerite with relatively minor inert impurities (10-20%). The substituted iron is estimated at 0.6 moles of Fe from the thermal diagram. The total iron analysis of 8.25% is consistent with this interpretation. 12-6 suggests 10% dolomite, 50% calcite and inerts. 12-7 is a reasonably pure ankerite containing about 1.00 moles of Fe. The total iron analysis was 13.9%. The slight peak at 880° C indicates some admixed dolomite.

12-8 is a rather pure calcite with 5% dolomite present. 12-9 appears to be an ankerite with about 0.5 moles of Fe. 10-20% of excess calcite seems present. The chemical analysis clearly indicates calcite mixing: CaO 38.28%, MgO 9.30%, FeO 9.29%, and CO₂ 44.20%. 12-10 shows 10-20% high iron ankerite with 50% calcite.

V. DISCUSSION

This study has thrown some light on the extent of substitution found among the common carbonate minerals. Figure 13 furnishes a trilinear plot of the data on samples whose mineral composition has been determined either in this study or elsewhere. The discontinuity between the calcite type of lattice (calcite, magnesite, and siderite) and the ankerite lattice is very striking. Apparently there is sufficient energy difference between randomly substituted Mg-Fe ions in the calcite lattice and an ordered (layered) structure, that in nature one or the other forms. Many of the specimens studied in this work were mixtures of lattices. This emphasizes the energy differential between the two structures. It is also clear that in the ankerite lattice Fe substitutes for Mg without any break but that there is negligible substitution of Mg or Fe in the Ca positions. Thus all of the ankerite specimens on which chemical data exist in this study fall on the horizontal line of 50% Ca. Complete substitution is observed between Fe⁺⁺ and Mg⁺⁺ but in the direction of Ca the substitution is restricted to about 10%. Likewise the few analyzed calcite specimens show little substitution. It is possible that some of the separation is due to the geochemical conditions of formation. However, the intimate intergrowth of siderite and calcite or siderite and ankerite suggests the main reason for the lack of more substitution is lattice potential energy differences.

In the study on rhodochrosite (Kulp, Wright, and Holmes, 1949),

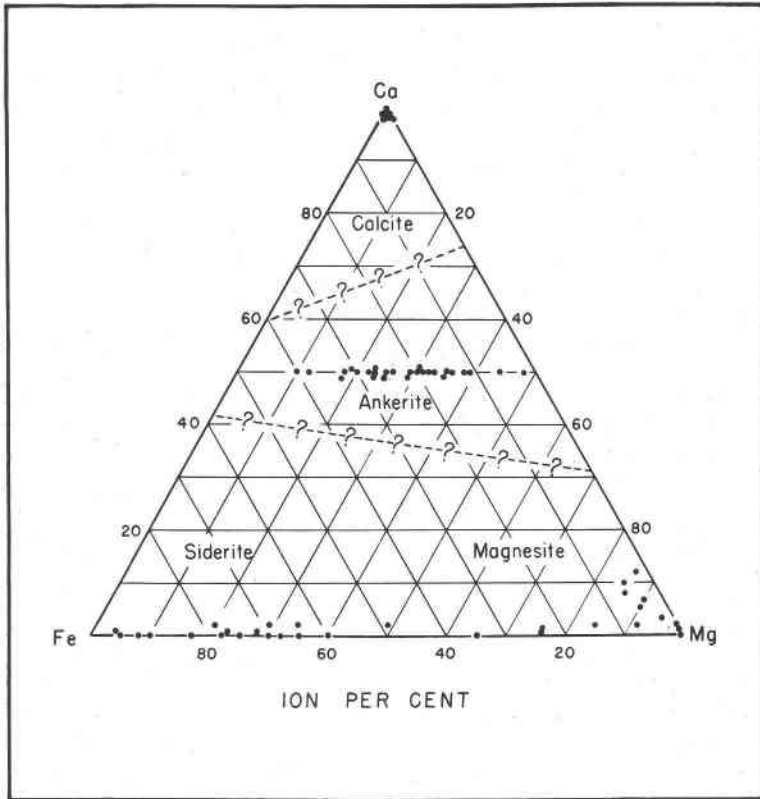


FIG. 13. Composition-phase diagram for Ca-Fe-Mg carbonates. Most of the specimens are taken from this study.

sufficient specimens were obtained to indicate the complete ionic substitution of Mn^{++} to Ca^{++} in nature. Minerals have also been reported which clearly indicate a similar series between Fe^{++} and Mn^{++} . The data are meagre with regard to the Mg-Mn series. This is probably due to the rarity of the individual minerals and the special geochemical conditions requisite to the formation of both being present at the same time. These relationships appear reasonable on the basis of the ionic radii of Ca^{++} 1.06; Mn^{++} 0.91; Fe^{++} 0.83; and Mg^{++} 0.78 Å.

The results presented above indicate the usefulness of thermal analysis in elucidating the mineral composition of natural carbonate aggregates. The peaks are so sensitive to substitution that it is possible to estimate the cation composition of each phase. The peaks are sufficiently large so that the method could be used to great advantage in the study of car-

bonate mineralization in the field. A portable DTA apparatus such as described by Hendricks et al. (1946) should be quite satisfactory for many types of field studies. Where rapid chemical and mineralogical data on carbonates are required, the thermal method offers many advantages.

REFERENCES

- BECK, C. W. (1950), Differential thermal analysis curves of carbonate minerals: *Am. Mineral.*, **35**, 985-1013.
- BRAGG, W. L. (1937), *Atomic Structure of Minerals*, Cornell University Press, Ithaca, New York.
- CUTBERT, F. L., AND ROWLAND, R. A. (1947), Differential thermal analysis of rare carbonate minerals: *Am. Mineral.*, **32**, 111-116.
- FAUST, G. T. (1944), Differentiation of magnesite from dolomite in concentrates and tailings: *Econ. Geol.*, **39**, 192-251.
- FAUST, G. T. (1949), Dedolomitization, and its relation to a possible derivation of a magnesium-rich hydrothermal solution: *Am. Mineral.*, **34**, 789-823.
- FAUST, G. T. (1950), Thermal analysis studies on carbonates—I. Aragonite and calcite: *Am. Mineral.*, **35**, 207-224.
- FREDRICKSON, A. F. (1948), Differential thermal curve of siderite: *Am. Mineral.*, **33**, 372-374.
- HENDRICKS, S. B., GOLDRICH, S. S., AND NELSON, R. A., (1946), On a portable differential thermal outfit: *Econ. Geol.*, **41**, 41.
- KERR, P. F., AND KULP, J. L. (1947), Differential thermal analyses of siderite: *Am. Mineral.*, **32**, 678.
- KERR, P. F., AND KULP, J. L. (1948), Multiple differential thermal analysis: *Am. Mineral.*, **33**, 387-419.
- KULP, J. L., AND KERR, PAUL F. (1949), Improved differential thermal analysis, *Am. Mineral.*, **34**, 839-844.
- KULP, J. L., WRIGHT, H. D., AND HOLMES, R. J. (1949), Thermal study of rhodochrosite: *Am. Mineral.*, **34**, 195-219.
- ROWLAND, R. A., AND JONAS, E. C. (1949), Variations in differential thermal analysis curves of siderite: *Am. Mineral.*, **34**, 550-558.

Manuscript received March 31, 1951.